
Variational DAG Estimation via State Augmentation With Stochastic Permutations

Edwin V. Bonilla
CSIRO's Data61

Pantelis Elinas
CSIRO's Data61

He Zhao
CSIRO's Data61

Maurizio Filippone
Statistics Program, KAUST

Vassili Kitsios
CSIRO's Environment

Terry O'Kane
CSIRO's Environment

Abstract

Estimating the structure of a Bayesian network, in the form of a directed acyclic graph (DAG), from observational data is a statistically and computationally hard problem with essential applications in areas such as causal discovery. Bayesian approaches are a promising direction for solving this task, as they allow for uncertainty quantification and deal with well-known identifiability issues. From a probabilistic inference perspective, the main challenges are (i) representing distributions over graphs that satisfy the DAG constraint and (ii) estimating a posterior over the underlying combinatorial space. We propose an approach that addresses these challenges by formulating a joint distribution on an augmented space of DAGs and permutations. We carry out posterior estimation via variational inference, where we exploit continuous relaxations of discrete distributions. We show that our approach performs competitively when compared with a wide range of Bayesian and non-Bayesian benchmarks on a range of synthetic and real datasets.

1 Introduction

Graphs are a common way of representing data, describing the elements (i.e., variables) of the corresponding system via nodes and their relationships via edges. They are useful for understanding, prediction and causal inference [25, Ch. 30]. Of particular interest to this paper are directed acyclic graphs (DAGs), i.e., graphs with directed edges and no cycles. Important application areas where DAGs find their place abound, for example in epidemiology [37], economics [18] genetics [36, 16] and biology [30].

However, estimating the structure of a DAG from observational data is a computationally and statistically hard problem. From the computational perspective, the space of DAGs grows super-exponentially in the dimensionality of the problem. From the statistical perspective, even in low-dimensional settings and with infinite data, one can only estimate the “true” underlying DAG up to the Markov equivalence class.

Learning DAG structures has, of course, been intensely studied in the machine learning and statistics literature [see, e.g., 27, 20] and has been shown to be an NP-hard problem [9]. The main difficulty being that of enforcing the acyclicity constraint in the underlying (discrete) combinatorial space. Fortunately, recent breakthroughs in continuous characterizations of the “dagness” constraint [46, 4] have shown much promise, opened up new directions and allowed addressing applications previously considered intractable [39].

Nevertheless, the above approaches do not model uncertainty explicitly. This is important for handling identifiability issues, the incorporation of prior knowledge, dealing with noise and solving

downstream tasks such as estimation of causal quantities [13]. Furthermore, as pointed out by [12], learning a single DAG structure may lead to confident but incorrect predictions [24].

Thus, in this paper we propose a probabilistic approach to learning DAG structures from observational data by adopting a Bayesian perspective. The main challenges that we address in this regard are: (i) *representational*: how to represent distributions over graphs that inherently satisfy the DAG constraint; and (ii) *computational*: how to estimate a posterior distribution over the underlying combinatorial space. Our solution tackles the representational challenge by formulating a joint distribution over an augmented space of DAGs and permutations. More specifically, we first model a distribution over node orderings and then formulate a conditional distribution over graphs that is consistent with the given order. This results in a valid general distribution over DAGs. To tackle the computational challenge, we resort to variational inference. For this we rely on reparameterizations and continuous relaxations of simple base distributions. We show that our method handles linear and non-linear models and performs competitively when compared against a wide variety of Bayesian and non-Bayesian benchmarks on a range of synthetic and real datasets.

2 Related work

Causal discovery: Causal discovery from observational data has also motivated the development of many algorithms for graph learning, with a lot of previous work framed under the assumption of linear structural equation models [see, e.g., 32, 33] but more general nonlinear approaches have also been proposed [17, 44]. Perhaps, one of the most well known methods for causal discovery is the PC algorithm [34], which is based on conditional independence tests. We refer the reader to the excellent review by [14] for more details on causal discovery methods.

Point estimation via continuous formulations: Within the machine learning literature, due to the NP-hardness nature of the problem [9], a lot of heuristics to deal with the combinatorial challenge have been proposed [see, e.g., 8]. This has motivated research for more tractable continuous formulations that allow for general function approximations to be applied along with gradient-based optimization [21, 40, 22, 2, 19, 43, 46, 4]. From these, the NOTEARS [46] and DAGMA [4] methods stand out, as they provide “exact” characterizations of acyclicity. These characterizations can be used as regularizers within optimization-based learning frameworks. However, they have a cubic-time complexity on the input dimensionality.

Linear Bayesian approaches: More critically, while all these advances provide a plethora of methods for DAG estimation, with the exception of [22], most of these approaches are not probabilistic and they lack inherent uncertainty estimation. Bayesian causal discovery nets [BCDNET, 10] address this limitation with a Bayesian model that, unlike ours, is limited to linear SEMs. Their approach is somewhat analogous to ours in that they propose a joint model over permutation and weight matrices. However, their variational distribution is fundamentally different, with distributions over permutation matrices based on Boltzmann distributions and inference involving an optimal transport problem, hence, requiring several downstream approximations for tractability.

Nonlinear Bayesian methods: Unlike BCDNET, and like ours, DIBS [22], DECI [13] and JSP-GFN [12] frameworks handle the more general nonlinear SEM setting. As described in Section 4, DIBS and DECI incorporate the NOTEARS characterization within their priors and, therefore, their posteriors do not inherently model distributions over DAGs. In contrast, using a very different formulation based on generative flow networks [5], [12] propose a method that learns the parameters of the graphical model and its structure jointly. Although underpinned by solid mathematical foundations, the performance of their method is hindered by the slow moves in the DAG space (“one edge at a time”), and may fail to discover reasonable structures from data under limited computational constraints.

Other state-augmentation approaches: Similar augmentation approaches for modeling DAGs probabilistically have been proposed recently. In particular, DDS [7] and DPM-DAG [29] also use permutation-based approaches, while BAYESDAG [1] proposes an augmentation based on “node potentials”, which is intriguingly related to permutation-based augmentations. While DDS does not propose joint probabilistic inference over adjacencies *and* permutations, DPM-DAG focuses on formulating and evaluating valid/sensible priors using the 2 mainstream methods: (1) Gibbs-like priors through continuous characterizations such as NOTEARS and (2) a permutation-based formulation. Moreover, they use categorical distributions over the permutation matrices, which does not yield a

valid evidence lower bound (ELBO) for Gumbel-softmax samples and continuous relaxations of the permutation matrix.

3 Problem set-up

We are given a matrix of observations $\mathbf{X} \in \mathbb{R}^{N \times D}$, representing N instances with D -dimensional features. Formally, we define a directed graph as a set of vertices and edges $\mathcal{G}_A = (\mathcal{V}, \mathcal{E})$ with D nodes $v_i \in \mathcal{V}$ and edges $(v_i, v_j) \in \mathcal{E}$, where an edge has a directionality and a weight associated with it. We use the adjacency matrix representation of a graph $\mathbf{A} \in \mathbb{R}^{D \times D}$, which is generally a sparse matrix with an entry $A_{ij} = 0$ indicating that there is no edge from vertex v_i to vertex v_j and $A_{ij} \neq 0$ otherwise. In the latter case, we say that node v_i is a parent of v_j . Generally, for DAGs, \mathbf{A} is not symmetric and subject to the acyclicity constraint. This means that if one was to start at a node v_i and follow any directed path, it would not be possible to get back to v_i .

Thus, we associate each variable x_i with a vertex v_i in the graph and denote the parents of x_i under the given graph \mathcal{G}_A with $\text{pa}(i; \mathcal{G}_A)$. Our goal is then to estimate \mathcal{G}_A from the given data, assuming that each variable is a function of its parents in the graph, i.e., $x_i = f_i(\mathbf{x}_{\text{pa}(i; \mathcal{G}_A)}) + z_i$, where z_i is a noise (exogenous) variable and each functional relationship $f_i(\cdot)$ is unknown¹. Importantly, since \mathcal{G}_A is a DAG, it is then subject to the acyclicity constraint. Due to the combinatorial structure of the DAG space, this constraint is what makes the estimation problem hard.

Under some strict conditions, the underlying “true” DAG generating the data is identifiable but not always; for example, even with infinite data and under low-dimensional settings, the true DAG is not identifiable in the simple linear-Gaussian case. Furthermore, learning a single DAG structure may be undesirable, as this may lead to confident but incorrect predictions [12, 24]. Furthermore, averaging over all possible explanations of the data may yield better performance in downstream tasks such as the estimation of causal effects [13]. Therefore, here we address the more general (and harder) problem of estimating a *distribution* over DAGs.

4 Representing distributions over DAGs

Recent advances such as NOTEARS [46] and DAGMA [4] formulate the structure DAG learning problem as a continuous optimization problem via smooth characterizations of acyclicity. This allows for the estimation of a single DAG within cleverly designed optimization procedures. In principle, one can use such characterizations within optimization-based probabilistic inference frameworks such as variational inference by encouraging the prior towards the DAG constraint. This is, in fact, the approach adopted by the deep end-to-end causal inference (DECI) method of [13]. However, getting these types of methods to work in practice is cumbersome and, more importantly, the resulting posteriors are not inherently distributions over DAGs. Here we present a simple approach to represent distributions over DAGs by augmenting our space of graphs with permutations.

4.1 Ordered-based representations of DAGs

A well-known property of a DAG is that its nodes can be sorted such that parents appear before children. This is usually referred to as a topological ordering [see, e.g., 25, §4.2]. This means that if one knew the true underlying ordering of nodes, it would be possible to draw arbitrary links from left to right while always satisfying acyclicity². Such a basic property can then be used to estimate DAGs from observational data. The main issue is that, in reality, one knows very little about the underlying true ordering of the variables, although in some applications this may be the case [26]. Nevertheless, this hints at a representation of DAGs in an augmented space of graphs and orderings/permutations.

¹In the sequel, we will refer to this set of equations as a structural equation model (SEM).

²In our implementation we actually use *reverse* topological orders. Obviously, this does not really matter as long as the implementation is consistent with that of the adjacency matrix.

5 DAG distributions in an augmented Space

The main idea here is to define a distribution over an augmented space of graphs and permutations. First we define a distribution over permutations and then we define a conditional distribution over graphs given that permutation. As we have described above, this gives rise to a very general way of generating DAGs and, consequently, distributions over them.

In the next section we will describe very simple distributions over permutations. As we shall see in Section 7, our proposed method is based on variational inference and, therefore, we will focus on two main operations: (1) being able to compute the log probability of a sample under our model and (2) being able to draw samples from that model. Henceforth, we will denote a permutation over D objects with $\pi = (\pi_1, \dots, \pi_D)$.

5.1 Distributions over permutations

We can define distributions over permutations by using Gamma-ranking models [35]. The main intuition is that we have a competition with D players, each having to score r points. We denote V_1, \dots, V_D the times until D independent players score r points. Assuming player j scores points according to a Poisson process with rate γ_j , then V_j has a Gamma distribution with shape parameter r and scale parameter γ_j . We are interested in the probability of the permutation $\pi = (\pi_1, \dots, \pi_D)$ in which object π_j has rank j .

Thus, $p(\pi | r, \gamma)$ is equivalent to the probability that $V_{\pi_1} < \dots < V_{\pi_D}$. with this, $\forall V_j > 0, r > 0, \gamma_j > 0$, we have that : $p(V_j) = \text{Gamma}(V_j; r, \gamma_j)$, $p(\pi | r, \gamma) = \Pr(V_{\pi_1} < \dots < V_{\pi_D})$, where $\text{Gamma}(v; r, \gamma) = \frac{1}{\Gamma(r)\gamma^r} v^{r-1} \exp\left(-\frac{v}{\gamma}\right)$ is the shape-scale parameterization of the Gamma distribution and $\Gamma(\cdot)$ is the Gamma function. The probability above is given by a high-dimensional integral that depends on the ratios between scales and, therefore, is invariant when multiplying all the scales by a positive constant. Consequently, it is customary to make $\sum_{j=1}^D \gamma_j = 1$.

Shape r=1: In the simple case of $r = 1$, V_j, \dots, V_D are drawn from D independent exponential distributions each with rate $1/\gamma_j$: $p(v_j | r = 1, \gamma_j) = \frac{1}{\gamma_j} \exp(-\frac{v_j}{\gamma_j})$. To understand the order distribution, we look at the distribution of the minimum. Lets define the random variable: $I = \arg \min_{i \in \{1, \dots, D\}} \{V_1, \dots, V_D\}$. We are interested in computing $\Pr(I = k)$, which can be shown to be $\Pr(I = k) = \frac{\beta_k}{\beta_1 + \dots + \beta_D}$, where $\beta_k := 1/\gamma_k$ is the rate parameter of the exponential distribution. See Appendix A for details.

5.1.1 Probability of a permutation

Thus, under the model above with independent exponential variables $p(v_j | r = 1, \beta_j) = \beta_j \exp(-\beta_j v_j)$, the log probability of a permutation (ordering) can be easily computed by calculating the probability of the first element being the minimum among the whole set, then the probability of the second element being the minimum among the rest (i.e., the reduced set without the first element) and so on:

$$p(\pi | r = 1, \beta) = \beta_{\pi_1} \left(\frac{\beta_{\pi_2}}{1 - \beta_{\pi_1}} \right) \left(\frac{\beta_{\pi_3}}{1 - \beta_{\pi_1} - \beta_{\pi_2}} \right) \times \dots \left(\frac{\beta_{\pi_D}}{1 - \sum_{j=1}^{D-1} \beta_{\pi_j}} \right), \quad (1)$$

and, therefore, we have that the log probability of a permutation under our model can be computed straightforwardly from above.

5.1.2 Sampling hard permutations

We can sample hard permutations from the above generative model by simply (1) generating draws from an exponential distribution $v_j \sim p(v_j | r = 1, \beta_j)$, $j = 1, \dots, D$: $z_j \sim \text{Uniform}(0, 1)$ $v_j = -\beta_j^{-1} \log(1 - z_j)$; and then (2) obtaining the indices from the sorted elements $\pi = \text{argsort}(\mathbf{v}, \text{descending}=\text{False})$, where the $\text{argsort}(\mathbf{v}, \text{descending}=\text{False})$ operation above returns the indices of the sorted elements of \mathbf{v} in ascending order. Alternative, we can also exploit Equation (1) and sample from this model using categorical distributions, see Appendix B.

We have purposely used the term *hard* permutations above to emphasize that we draw actual discrete permutations. In practice, we represent these permutations via binary matrices $\mathbf{\Pi}$, as described in Appendix D.4. However, in order to back-propagate gradients we need to relax the `argsort` operator.

5.1.3 Soft permutations via relaxations and alternative constructions

We have seen that sampling from our distributions over permutations requires the `argsort` operator which is not differentiable. Therefore, in order to back-propagate gradients and estimate the parameters of our models, we relax this operator following the approach of [28], see details in Appendix F. Furthermore, the probabilistic model in Equation (1) can be seen as an instance of the Plackett-Luce model. Interestingly, [42] has shown that the Plackett-Luce model can only be obtained via a Gumble-Max mechanism, implying that both approaches should be equivalent. Details of this mechanism are given in Appendix C but, essentially, both constructions (the Gamma/Exponential-based sampling process and the Gumble-Max mechanism) give rise to the same distribution.

5.2 Conditional distribution over DAGs given a permutation

In principle, this distribution should be defined as conditioned on a permutation π and, therefore, have different parameters for every permutation. In other words, we should have $p(\mathcal{G}_A | \theta_\pi)$, where θ_π are permutation-dependent parameters. This is obviously undesirable as we would have $D!$ parameter sets. In reality, we know we can parameterize general directed graphs using “only” $O(D^2)$ parameters, each corresponding to the probability of a link between two different nodes $i, j \forall i, j \in \{1, \dots, D\}, i \neq j$. Considering only DAGs just introduces additional constraints on the types of graphs we can have. Thus, WLOG, we will have a global vector θ of $D(D - 1)$ parameters³, and θ_π are obtained by simply extracting the corresponding subset that is consistent with the given permutation. See details of the implementation in Appendix D.5.

5.2.1 Probability of a DAG given a permutation

Given a permutation $\pi = (\pi_1, \dots, \pi_D)$, the probability (density) of a graph \mathcal{G}_A represented by its adjacency matrix \mathbf{A} can be defined as:

$$p(\mathcal{G}_A | \pi, \Theta) = \prod_{k'=1}^D \prod_{k=k'+1}^D p_\pi(A_{\pi_k \pi_{k'}} | \Theta_{\pi_k \pi_{k'}}), \quad (2)$$

where $p_\pi(A_{\pi_k \pi_{k'}} | \Theta_{\pi_k \pi_{k'}})$ is a base link distribution with parameter $\Theta_{\pi_k \pi_{k'}}$, $\mathcal{G}_A \in \mathbb{G}_\pi$, and \mathbb{G}_π is the set of graphs *consistent* with permutation π (Appendix D.5). Conceptually, we constrain all the possible graphs that could have been generated with this permutation. In other words, the distribution is over the graphs the given permutation constrain the model to consider. More importantly, we will see that in our variational scheme in Section 7, we will never sample a graph inconsistent with the permutation (as we will always do this conditioned on the given permutation). Therefore, the computation above is always well defined.

There are a multitude of options for the base link distribution depending on whether we want to model binary or continuous adjacency matrices; how they interact with the structural equation model (SEM); and for example, how we want to model sparsity. In Appendix E we give full details of the Relaxed Bernoulli distribution but our implementation supports other densities such as Gaussian and Laplace.

5.2.2 Sampling from a DAG given a permutation

Given a permutation $\pi = (\pi_1, \dots, \pi_D)$ we sample a DAG and adjacency \mathbf{A} with underlying parameter matrix Θ as: for $k' = 1, \dots, D$ and $k = k' + 1, \dots, D$ $A_{\pi_k \pi_{k'}} \sim p_\pi(\Theta_{\pi_k \pi_{k'}})$. Clearly, as the conditional distribution of a DAG given a permutation factorizes over the individual links, the above procedure can be readily parallelized and our implementation exploits this.

³This just considers all possible links except self-loops. It is possible, although not considered in this work, to drastically reduce the number of parameters by using *amortization*.

6 Full joint distribution

We define our joint model distribution over observations \mathbf{X} , latent graph structures \mathcal{G}_A and permutations π as

$$p(\mathbf{X}, \mathcal{G}_A, \pi | \psi) = p(\pi | r_0, \beta_0) p(\mathcal{G}_A | \pi, \Theta_0) \prod_{n=1}^N p(\mathbf{x}^{(n)} | \mathcal{G}_A, \phi), \quad (3)$$

where the joint prior $p(\pi | r_0, \beta_0)$ and $p(\mathcal{G}_A | \pi, \Theta_0)$ are given by Equation (1) and Equation (2), respectively; $\psi = \{r_0, \beta_0, \Theta_0, \}$ are model hyper-parameters; and $p(\mathbf{x}^{(n)} | \mathcal{G}_A, \phi)$ is the likelihood of a structural equation model, with parameters ϕ , satisfying the parent constraints given by the graph \mathcal{G}_A as described below.

Likelihood of structural equation model: we investigate additive noise models giving rise to a conditional likelihood of the form $p(\mathbf{x} | \mathcal{G}_A, \phi) = \prod_{j=1}^D p_{z_j}(x_j - f_j(\mathbf{x}_{\text{pa}(j; \mathcal{G}_A)}))$, where $\text{pa}(i; \mathcal{G}_A)$ denotes the parents of variable x_i and $p_{z_i}(z_i) = \text{Normal}(z_i; 0, \sigma^2)$. While the linear case is straightforward, the nonlinear case cannot use a generic neural network, as the architecture must satisfy the parent constraints by the graph \mathcal{G}_A . In our experiments, we use the graph conditioner network proposed by [41].

7 Posterior estimation

Our main latent variables of interest are the permutation π constraining the feasible parental relationships and the graph \mathcal{G}_A fully determined by the adjacency matrix \mathbf{A} . In the general case, exact posterior estimation is clearly intractable due to the nonlinearities inherent to the model and the marginalization over a potentially very large number of variables. Here we resort to variational inference that also allows us to represent posterior over graphs *compactly*.

7.1 Variational distribution

Similar to our joint prior over permutations and DAGs, our approximate posterior is given by:

$$q_{\lambda}(\pi, \mathcal{G}_A) = q_{\pi}(\pi | r, \beta) q_{\mathcal{G}}(\mathcal{G}_A | \pi, \Theta), \quad (4)$$

which have the same functional forms as those in Equation (1) and Equation (2). Henceforth, we will denote the variational parameters with $\lambda := \{\beta, \Theta\}$.

7.2 Evidence lower bound

The evidence lower bound (ELBO) is given by:

$$\mathcal{L}_{\text{ELBO}}(\lambda) = -\text{KL}[q_{\lambda}(\pi, \mathcal{G}_A) \| p(\pi, \mathcal{G}_A | \beta_0, \Theta_0)] + \mathbb{E}_{q_{\lambda}(\pi, \mathcal{G}_A)} \sum_{n=1}^N \log p(\mathbf{x}^{(n)} | \mathcal{G}_A, \phi), \quad (5)$$

where $\text{KL}[q \| p]$ denotes the KL divergence between distributions q and p and \mathbb{E}_q denotes the expectation over distribution q . we note we can further decompose the KL term as:

$$\begin{aligned} \text{KL}[q_{\lambda}(\pi, \mathcal{G}) \| p(\pi, \mathcal{G}_A | \beta_0, \Theta_0)] &= \mathbb{E}_{q_{\pi}(\pi | r, \beta)} \left[\log q_{\pi}(\pi | r, \beta) - \log p(\pi | r_0, \beta_0) + \right. \\ &\quad \left. \mathbb{E}_{q_{\mathcal{G}_A}(\mathcal{G}_A | \pi, \Theta)} [\log q_{\mathcal{G}_A}(\mathcal{G}_A | \pi, \Theta) - \log p(\mathcal{G}_A | \pi, \Theta_0)] \right]. \quad (6) \end{aligned}$$

We estimate the expectations using Monte Carlo, where samples are generated as described in Sections 5.1.2 and 5.2.2 and the log probabilities are evaluated using Equations (1) and (2). Here we see we need to back-propagate gradients wrt samples over distributions on permutations, as described in Section 5.1.2. For this purpose, we use the relaxations described in Section 5.1.3.

In practice, one simple way to do this is to project the samples onto the discrete permutation space in the forward pass and use the relaxation in the backward pass, similarly to how Pytorch deals

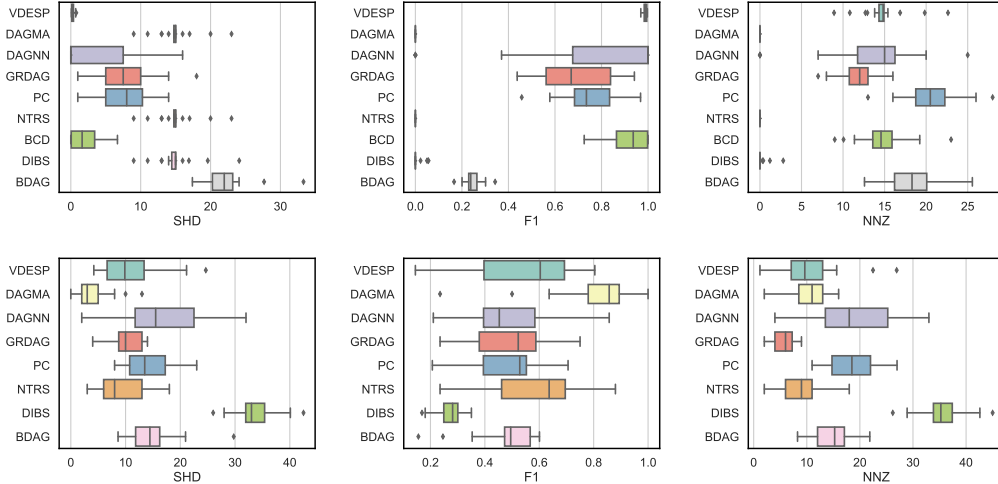


Figure 1: Results on synthetic linear (top) and nonlinear (bottom) data. The structural Hamming distance (SHD, the lower the better); the F1 score (the higher the better); and the number of non-zeros (NNZ, the closer to $\bar{E} = 16$ the better) with $D = 16$ and on all graphs. The results for DECI, JSP-GFN and DDS were too poor and, consequently, not shown here. GRANDAG, NOTEARS, BCDNET and BAYESDAG are referred to as GRDAG, NTRS, BCD and BDAG respectively.

with Relaxed Bernoulli (also known as Concrete) distributions. Sometimes this is referred to as a straight-through estimator⁴.

Furthermore, we note that our models for the conditional distributions over graphs given a permutation do not induce strong sparsity and, therefore, they will tend towards denser DAGs. We obtain some kind of parsimonious representations via quantization and early stopping during training. However, to maintain the soundness of the objective, as pointed out by [23] in the context of Concrete distributions, the KL term is computed in the unquantized space.

Finally, in the non-linear SEM case, we also need to estimate the parameters of the corresponding neural network architecture. We simply learn these jointly along with the variational parameters by optimizing the ELBO in Equation (5). For simplicity in the notation, we have omitted the dependency of the objective on these parameters.

8 Experiments & results

We evaluate our approach on several synthetic, pseudo-real and real datasets used in the previous literature, comparing with competitive baseline algorithms under different metrics. In particular, we compare our method with BCDNET [10], DAGMA [4], DAGGNN [43], GRANDAG [19], NOTEARS [46], DECI [13], JSP-GFN [12], DIBS [22], DDS [7] and BAYESDAG [1]. The results for DECI, JSP-GFN and DDS are not shown in the figures, as they were found to underperform all the competing algorithms significantly (making the figures difficult to read), underlying the challenging nature of the problems we are addressing, especially in the nonlinear SEM case. This is discussed in the text in Section 8.1.

Metrics: As evaluation metrics we use the structural Hamming distance (SHD), which measures the number of changes (edge insertions/deletions/directionality change) needed in the predicted graph to match the underlying true graph. We also report the F1 score, measured when formulating the problem as that of classifying links including directionality, and the number of non-zeros (NNZ) in the predicted adjacencies. We emphasize here that there is no perfect metric for our DAG estimation task and one usually should consider several metrics jointly. For example, we have found that some

⁴However, we still use the relaxation in the forward pass, which is different from the original estimator proposed in [6]. We also note that the Pytorch implementation of their gradients is a mixture of the Concrete distributions approach and the straight-through estimator.

methods have the tendency to predict very sparse graphs and will obtain very low SHDs when the number of links in the underlying true graph is also very sparse. This will be reflected in other metrics such as NNZ. At the end of the section, we also evaluate uncertainty quantification across the Bayesian methods.

Algorithm settings: For BCDNET, DECI, JSP-GFN, DIBS, BAYESDAG and DDS we used the implementation provided by the authors. For all the other baseline algorithms we used GCASTLE [45]. Hyper-parameter setting was followed from the reference implementation and the recommendation by the authors (if any) in the original paper. However, for JSP-GFN we did try several configurations for their prior and model, none of which gave us significant performance improvements subject to our computational constraints (hours for each experiment instead of days).

For our algorithm (VDESP) we set the prior and posteriors to be Gaussians, used a link threshold for quantization of 0.5. For experiments other than the synthetic linear, we used a non-linear SEM as described in Section 6, i.e., based on a Gaussian exogenous noise model and the proposed architecture in [41] and learned its parameters via gradient-based optimization of the ELBO. Please see appendix for full details.

8.1 Synthetic data

Linear datasets: Here we follow a similar setting to that of [13] and generate Erdős-Rényi (ER) graphs and scale-free (SF) graphs as described in [19, §A.5] where the SF graphs follow the preferential attachment model of [3]. We use $D = 16$ nodes, $\bar{E} \in \{16, 64\}$ expected edges and $N = 1000$. We used a linear Gaussian SEM with the corresponding weights set to 1, biases to 0, mean zero and variance 0.01. Experiments were replicated 10 times.

The results across all graphs (ER and SF) are shown in Figure 1 (top). We see that our method VDESP performs the best among all competing approaches both in terms on the SHD and the F1 score. VDESP’s posterior exhibits a small variance, showing its confidence on its closeness to the underlying true graph. BCDNET performs very well too, given that it was specifically design for linear SEMs. Surprisingly, DAGMA performs poorly perhaps indicating the hyper-parameters used were not adequate for this dataset. Additional results with a larger number of edges and separate for ER and SF graphs can be found in Appendix H.

Nonlinear datasets: Here we adopted a similar approach to the synthetic linear dataset now with $D = 16$, $\bar{E} = 16$, $N = 1000$, a nonlinear SEM given by a MLP with a noise model with mean zero and variance 1. Results are shown in Figure 1, where we note that we have not included BCDNET, as this method was not designed to work on nonlinear SEMs. We see that VDESP is marginally better than DAGGNN, GRANDAG and performs similarly to NOTEARS, while DAGMA achieves the best results on average. However, as mentioned throughout this paper, VDESP is much more informative as it provides a full posterior distribution over DAGs. We believe the fact that VDESP is competitive here is impressive as it is learning both a posterior over the DAG structure as well as the parameters of the nonlinear SEM [using the architecture proposed by 41].

We also emphasize that we evaluated other Bayesian nonlinear approaches such as DECI, JSP-GFN and DDS but their results were surprisingly poor in terms of SHD and F1. This only highlights the challenges of learning a nonlinear SEM along with the DAG structure. However, it is possible that under a lot more tweaking of their hyper-parameters (for which we have very little guidance) and much larger computational constraints, one can get them to achieve comparable performance. More detailed results of this nonlinear setting are given in Appendix H.

8.2 Pseudo-real & real datasets

SYNTREN: This pseudo-real dataset was used by [19] and generated using the SynTReN generator of [38]. The data represent genes and their level of expression in transcriptional regulatory networks. The generated gene expression data approximates experimental data. It has 10 sets of $N = 500$ observations, $D = 20$ variables and $\bar{E} = 33.3$ edges.

DREAM4: This real dataset is from the Dream4 in-silico network challenge on gene regulation as used previously by [2]. We use the multi-factorial dataset with $D = 10$ nodes and $N = 10$ observations of which we have 5 different sets of observations and ground truth graphs, with $\bar{E} = 14.2$ edges.

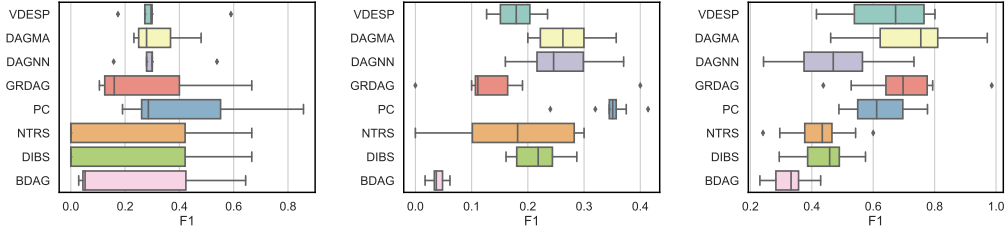


Figure 2: Results on real datasets: DREAM4 (Left), SACHS (middle) and SYNTREN (right). The F1 score (the higher the better) computed on the classification problem of predicting links including directionality. See Figure 6 in the appendix for SHD values. Method names as in Figure 1.

SACHS: This real dataset is concerned with the discovery of protein signaling networks from flow cytometry data as described in [30] with $D = 11$ variables, $N = 4,200$ observations with 10 different sets of observations and ground truth graphs, with $\bar{E} = 17.0$ edges.

Results are shown in Figure 2. On these datasets we have assumed that one has very little knowledge of the underlying SEM and, therefore, as with the synthetic nonlinear data, we have excluded BCDNET. We see that VDESP performs competitively in terms of F1 across datasets and can outperform other state-of-the-art Bayesian methods such as BAYESDAG, while providing competitive SHD values throughout, even clearly outperforming DAGMA and DAGGNN on DREAM4 (top left of Figure 6 in the appendix) and DAGGNN on SYNTREN (top right of Figure 6 in the appendix).

Understanding Alzheimer’s disease: Alzheimer’s disease (AD) is a degenerative brain disease and the most common form of dementia. It is estimated that around 55 million people are living with AD worldwide⁵. The public health, social and economic impact of AD is, therefore, an important problem. We used VDESP to understand the progression and diagnosis of the disease. Overall, VDESP’s predictions uncovered what is known to be the “gold standard” for relationships between AD biomarkers and cognition while, using samples from the posterior, hinting at interesting alternative explanations of the disease. See Appendix I for details.

Uncertainty quantification

One of the advantages of Bayesian methods over single-point estimation approaches is that they allow for uncertainty quantification. For the problem of DAG estimation we are interested in evaluating how well calibrated are the predicted marginal link probabilities of the underlying graph. To this end, we compute the expected calibration error (ECE) as: $ECE = \sum_{m=1}^M \frac{|B_m|}{N} |\text{acc}(B_m) - \text{conf}(B_m)|$, where $\text{acc}(B_m)$ and $\text{conf}(B_m)$ are the average accuracy and confidence (i.e., predicted probability) on bin m and the average is taken across M bins each of size $|B_m|$. Figure 3 illustrates how the different methods compare on this metric, where we see clearly that VDESP outperforms recently proposed competitive Bayesian methods such as BAYESDAG. However, due to the highly sparse nature of the problem, we note that this metric must not be taken in isolation but in conjunction with the previously reported metrics. Indeed, although DIBS appears to be performing well on this metric, the results on Figure 1 indicate that it performs poorly overall.

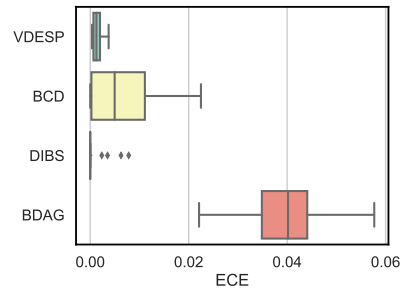


Figure 3: Expected calibration error on synthetic data.

⁵https://www.alz.org/alzheimer_s_dementia.

9 Conclusion, limitations and future work

We have presented a Bayesian DAG structure estimation method that inherently encodes the acyclicity constraint by construction on its model (and posterior) distributions. It does so by considering joint distributions on an augmented space of permutations and graphs. Given a node ordering sampled from a permutation distribution, our model defines simple and consistent distributions over DAGs. We have developed a variational inference method for estimating the posterior distribution over DAGs and have shown that it can outperform competitive benchmarks across a variety of synthetic, pseudo-real and real problems. As currently implemented, VDESP does come with its own limitations. In particular, we believe that incorporating better prior knowledge through strongly sparse and/or hierarchical distributions may make our method much more effective. We will explore this direction in future work.

References

- [1] Yashas Annadani, Nick Pawlowski, Joel Jennings, Stefan Bauer, Cheng Zhang, and Wenbo Gong. BayesDAG: Gradient-Based Posterior Inference for Causal Discovery. In *NeurIPS*, 2023.
- [2] Yashas Annadani, Jonas Rothfuss, Alexandre Lacoste, Nino Scherrer, Anirudh Goyal, Yoshua Bengio, and Stefan Bauer. Variational causal networks: Approximate Bayesian inference over causal structures. *arXiv preprint arXiv:2106.07635*, 2021.
- [3] Albert-László Barabási. Scale-free networks: A decade and beyond. *Science*, 325(5939):412–413, 2009.
- [4] Kevin Bello, Bryon Aragam, and Pradeep Ravikumar. DAGMA: Learning DAGs via M-matrices and a Log-Determinant Acyclicity Characterization. Number Neural Information Processing Systems, 2022.
- [5] Yoshua Bengio, Salem Lahlou, Tristan Deleu, Edward J Hu, Mo Tiwari, and Emmanuel Bengio. Gflownet foundations. *Journal of Machine Learning Research*, 24(210):1–55, 2023.
- [6] Yoshua Bengio, Nicholas Léonard, and Aaron Courville. Estimating or Propagating Gradients Through Stochastic Neurons for Conditional Computation. *arXiv preprint arXiv:1308.3432*, pages 1–12, 2013.
- [7] Bertrand Charpentier, Simon Kibler, and Stephan Günnemann. Differentiable Dag Sampling. *ICLR 2022 - 10th International Conference on Learning Representations*, (2):1–25, 2022.
- [8] David Maxwell Chickering. Optimal structure identification with greedy search. *Journal of machine learning research*, 3(Nov):507–554, 2002.
- [9] Max Chickering, David Heckerman, and Chris Meek. Large-sample learning of bayesian networks is np-hard. *Journal of Machine Learning Research*, 5:1287–1330, 2004.
- [10] Chris Cundy, Aditya Grover, and Stefano Ermon. BCD Nets: Scalable Variational Approaches for Bayesian Causal Discovery. *Advances in Neural Information Processing Systems*, 9(NeurIPS):7095–7110, 2021.
- [11] Aramakis Dallakyan and Mohsen Pourahmadi. Learning Bayesian Networks through Birkhoff Polytope: A Relaxation Method. pages 1–10, 2021.
- [12] Tristan Deleu, Mizu Nishikawa-Toomey, Jithendaraa Subramanian, Nikolay Malkin, Laurent Charlin, and Yoshua Bengio. Joint Bayesian Inference of Graphical Structure and Parameters with a Single Generative Flow Network. In *NeurIPS*, 2023.
- [13] Tomas Geffner, Javier Antoran, Adam Foster, Wenbo Gong, Chao Ma, Emre Kiciman, Amit Sharma, Angus Lamb, Martin Kukla, Nick Pawlowski, et al. Deep end-to-end causal inference. *arXiv preprint arXiv:2202.02195*, 2022.
- [14] Clark Glymour, Kun Zhang, and Peter Spirtes. Review of causal discovery methods based on graphical models. *Frontiers in Genetics*, 10(JUN):1–15, 2019.

- [15] Aditya Grover, Eric Wang, Aaron Zweig, and Stefano Ermon. Stochastic optimization of sorting networks via continuous relaxations. In *7th International Conference on Learning Representations, ICLR 2019*, pages 1–23, 2019.
- [16] Sung Won Han, Gong Chen, Myun-Seok Cheon, and Hua Zhong. Estimation of directed acyclic graphs through two-stage adaptive lasso for gene network inference. *Journal of the American Statistical Association*, 111(515):1004–1019, 2016.
- [17] Patrik Hoyer, Dominik Janzing, Joris M Mooij, Jonas Peters, and Bernhard Schölkopf. Nonlinear causal discovery with additive noise models. *Advances in neural information processing systems*, 21, 2008.
- [18] Guido W Imbens. Potential outcome and directed acyclic graph approaches to causality: Relevance for empirical practice in economics. *Journal of Economic Literature*, 58:1129–1179, 2020.
- [19] Sébastien Lachapelle, Philippe Brouillard, Tristan Deleu, and Simon Lacoste-Julien. Gradient-Based Neural DAG Learning. (2018):1–23, 2019.
- [20] S L Lauritzen and D J Spiegelhalter. Local computations with probabilities on graphical structures and their application to expert systems. *Journal of the Royal Statistical Society: Series B (Methodological)*, 50:157–224, 1988.
- [21] Phillip Lippe, Taco Cohen, and Efstratios Gavves. Efficient neural causal discovery without acyclicity constraints. *arXiv preprint arXiv:2107.10483*, 2021.
- [22] Lars Lorch, Jonas Rothfuss, Bernhard Schölkopf, and Andreas Krause. DiBS: Differentiable Bayesian Structure Learning. *Advances in Neural Information Processing Systems*, 29(NeurIPS):24111–24123, 2021.
- [23] Chris J. Maddison, Andriy Mnih, and Yee Whye Teh. The concrete distribution: A continuous relaxation of discrete random variables. *5th International Conference on Learning Representations, ICLR 2017 - Conference Track Proceedings*, pages 1–20, 2017.
- [24] David Madigan, Jonathan Gavrin, and Adrian E Raftery. Enhancing the predictive performance of bayesian graphical models. 1994.
- [25] Kevin P Murphy. *Probabilistic Machine Learning*. MIT Press, Cambridge, MA, USA, 2023.
- [26] Yang Ni, Francesco C Stingo, and Veerabhadran Baladandayuthapani. Bayesian graphical regression. *Journal of the American Statistical Association*, 114:184–197, 2019.
- [27] Judea Pearl. *Probabilistic Reasoning in Intelligent Systems*. Morgan Kaufmann, San Francisco, CA, USA, 1988.
- [28] Sebastian Prillo and Julian Eisenschlos. SoftSort: A continuous relaxation for the argsort operator. In Hal Daumé III and Aarti Singh, editors, *Proceedings of the 37th International Conference on Machine Learning*, volume 119 of *Proceedings of Machine Learning Research*, pages 7793–7802. PMLR, 13–18 Jul 2020.
- [29] Simon Rittel and Sebastian Tschiatschek. Specifying prior beliefs over dags in deep bayesian causal structure learning. In *26th European Conference on Artificial Intelligence ECAI 2023*, September 2023.
- [30] Karen Sachs, Omar Perez, Dana Pe’er, Douglas A Lauffenburger, and Garry P Nolan. Causal protein-signaling networks derived from multiparameter single-cell data. *Science*, 308(5721):523–529, 2005.
- [31] Xinpeng Shen, Sis Ma, Prashnithi Vemuri, Gyurgy Simon, and the Alzheimer’s Disease Neuroimaging Initiative. Challenges and opportunities with causal discovery algorithms: Application to alzheimer’s pathophysiology. *Scientific Reports*, 10, 2020.
- [32] Shohei Shimizu, Patrik O Hoyer, Aapo Hyvärinen, Antti Kerminen, and Michael Jordan. A linear non-gaussian acyclic model for causal discovery. *Journal of Machine Learning Research*, 7(10), 2006.

- [33] Shohei Shimizu, Takanori Inazumi, Yasuhiro Sogawa, Aapo Hyvärinen, Yoshinobu Kawahara, Takashi Washio, Patrik O. Hoyer, and Kenneth Bollen. DirectLiNGAM: A direct method for learning a linear non-gaussian structural equation model. *Journal of Machine Learning Research*, 12:1225–1248, 2011.
- [34] Peter Spirtes, Clark N Glymour, and Richard Scheines. *Causation, prediction, and search*. MIT press, 2000.
- [35] Hal Stern. Models for distributions on permutations. *Journal of the American Statistical Association*, 85(410):558–564, 1990.
- [36] Chengwei Su, Angeline Andrew, Margaret R Karagas, and Mark E Borsuk. Using bayesian networks to discover relations between genes, environment, and disease. *BioData mining*, 6(1):1–21, 2013.
- [37] Peter W G Tennant, Eleanor J Murray, Kellyn F Arnold, Laurie Berrie, Matthew P Fox, Sarah C Gadd, Wendy J Harrison, Claire Keeble, Lysie R Ranker, Johannes Textor, Georgia D Tomova, Mark S Gilthorpe, and George T H Ellison. Use of directed acyclic graphs (dags) to identify confounders in applied health research: Review and recommendations. *International Journal of Epidemiology*, 50:620–632, 2021.
- [38] Tim Van den Bulcke, Koenraad Van Leemput, Bart Naudts, Piet van Remortel, Hongwu Ma, Alain Verschoren, Bart De Moor, and Kathleen Marchal. Syntren: a generator of synthetic gene expression data for design and analysis of structure learning algorithms. *BMC bioinformatics*, 7:1–12, 2006.
- [39] Matthew J Vowels, Necati Cihan Camgoz, and Richard Bowden. D’ya like dags? a survey on structure learning and causal discovery. *ACM Computing Surveys*, 55:1–36, 2022.
- [40] Benjie Wang, Matthew R Wicker, and Marta Kwiatkowska. Tractable uncertainty for structure learning. In Kamalika Chaudhuri, Stefanie Jegelka, Le Song, Csaba Szepesvari, Gang Niu, and Sivan Sabato, editors, *Proceedings of the 39th International Conference on Machine Learning*, volume 162 of *Proceedings of Machine Learning Research*, pages 23131–23150. PMLR, 17–23 Jul 2022.
- [41] Antoine Wehenkel and Gilles Louppe. Graphical normalizing flows. In Arindam Banerjee and Kenji Fukumizu, editors, *Proceedings of The 24th International Conference on Artificial Intelligence and Statistics*, volume 130 of *Proceedings of Machine Learning Research*, pages 37–45. PMLR, 13–15 Apr 2021.
- [42] John I. Yellott. The relationship between Luce’s Choice Axiom, Thurstone’s Theory of Comparative Judgment, and the double exponential distribution. *Journal of Mathematical Psychology*, 15(2):109–144, 1977.
- [43] Yue Yu, Jie Chen, Tian Gao, and Mo Yu. DAG-GNN: DAG structure learning with graph neural networks. *36th International Conference on Machine Learning, ICML 2019*, 2019-June:12395–12406, 2019.
- [44] K Zhang and A Hyvärinen. On the identifiability of the post-nonlinear causal model. In *25th Conference on Uncertainty in Artificial Intelligence (UAI 2009)*, pages 647–655. AUAI Press, 2009.
- [45] Keli Zhang, Shengyu Zhu, Marcus Kalander, Ignavier Ng, Junjian Ye, Zhitang Chen, and Lujia Pan. gcastle: A python toolbox for causal discovery, 2021.
- [46] Xun Zheng, Bryon Aragam, Pradeep Ravikumar, and Eric P. Xing. Dags with no tears: Continuous optimization for structure learning. *Advances in Neural Information Processing Systems*, 2018-Decem(1):9472–9483, 2018.

A Distribution of the Minimum in the Gamma/Exponential Model

We are interested in computing $\Pr(I = k)$ so we have

$$\Pr(I = k) = \int_0^\infty p(V_k = v) \Pr(\forall_{i \neq k} V_i > v) dv, \quad (7)$$

$$= \int_0^\infty p(V_k = v) \prod_{i \neq k} (1 - F_i(v)) dv, \quad (8)$$

where $p(V_k = v)$ is the exponential distribution defined in Section 5.1 and $F_i(v)$ is the cumulative distribution function of V_i . When each of the variables follows an exponential distribution as given by Section 5.1, we have that:

$$\Pr(I = k) = \frac{1}{\gamma_k} \int_0^\infty \exp\left(-\frac{v}{\gamma_k}\right) \prod_{i \neq k} \exp\left(-\frac{v}{\gamma_i}\right) dx \quad (9)$$

$$= \frac{1}{\gamma_k} \int_0^\infty \exp\left(-\sum_{i=1}^N \frac{1}{\gamma_i} v\right) dv \quad (10)$$

$$= \frac{\beta_k}{\beta_1 + \dots + \beta_N}, \quad (11)$$

B Alternative Sampling of Permutations from the Gamma Model

As explained in the main paper, we can also sample from this model by using categorical distributions based on Equation (1). In this case we simply sample from categorical distributions one at a time on a reduced set (which will give us the argmin on the reduced set):

1. Set $\mathcal{B} = \{\beta_1, \dots, \beta_D\}$ with $\beta_j \in \mathcal{B}$
2. For $i = 0, \dots, D - 1$
 - (a) Sample element π_i from a categorical distribution with parameters $\{\theta_k\}_{k=1}^{|\mathcal{B}|}$, $\theta_k = \frac{\beta_k}{\sum_j \beta_j}$ with $\beta_j \in \mathcal{B}$ ⁶
 - (b) Set $\mathcal{B} = \mathcal{B} - \{\pi_i\}$

C Gumbel-Max Constructions of Distributions over Permutations

Here we describe the Gumbel-Max construction of distributions over permutations, as given, e.g., in [15]. this construction is parameterized by a vector of log scores \mathbf{s} , which are corrupted with noise drawn from a Gumbel distribution. The resulting corrupted scores are then sorted in descending order as follows:

1. Let \mathbf{s} be a vector of scores
2. Sample g_i from a Gumbel distribution with location $\mu = 0$ and scale $\sigma > 0$
 - (a) $z_i \sim \text{Uniform}(0, 1)$
 - (b) $g_i = \mu - \sigma \log(-\log(z_i))$
3. Let $\tilde{\mathbf{s}}$ be the vector of perturbed scores with Gumbel noise such that:

$$\tilde{s}_i = \sigma \log s_i + g_i$$
4. $\boldsymbol{\pi} = \text{argsort}(\tilde{\mathbf{s}}, \text{descending}=\text{True})$,

where we emphasize the corrupted scores are sorted in descending order. As we will see below, the distribution over permutations generated with the above procedure is given by the RHS of Equation (1) with $\boldsymbol{\beta} = \mathbf{s}$. In our experiments, we use $\sigma = 1$.

⁶Here we note the need to re-normalize at every iteration to have a proper distribution even under the assumption $\sum_{j=1}^D \beta_j = 1$, which is only valid in the first iteration. We also note that, as we iteratively reduce the set \mathcal{B} , we need to keep track of the remaining elements to sample from.

C.1 Relation to Gamma Construction

Here we compare our Gumbel-Max construction with the Gamma/exponential construction described in Section 5.1.2 (based on the model proposed in [35]). This is interesting because [42] has shown that the Plackett-Luce model can only be obtained via the Gumble-Max mechanism, implying that both approaches should be equivalent.

It is shown in [42] that the distribution over permutations generated by the above procedure with *identical Gumbel scales* σ is given by Equation (1) with $\beta = \mathbf{s}$. This means that, essentially, our Exponential-based sampling process in Section 5.1.2 is equivalent to the one above. To show this, let us retake our Exponential samples (before the `argsort` operation):

$$x_i = -\beta_i^{-1} \log(1 - z_i) \quad (12)$$

$$= -\beta_i^{-1} \log(z_i), \quad (13)$$

as $1 - z_i \sim \text{Uniform}(0, 1)$. Now we (i) make $s_i := \beta_i$; (ii) take a log transform of the above variable, which is a monotonic transformation and preserves ordering; and (iii) multiply by $-\sigma$ so that we reverse the permutation to descending order:

$$-\sigma \log(x_i) = -\sigma \log(\beta_i^{-1} (-\log z_i)), \quad (14)$$

$$= \sigma \log s_i - \sigma \log(-\log z_i), \quad (15)$$

$$= \tilde{s}_i, \quad (16)$$

giving us exactly the noisy scores of the Gumbel-Max construction above. Presumably, this parameterization is more numerically stable as we are taking the log twice.

More generally, we can show that we can transform a Gumbel-distributed variable $g \sim \text{Gumbel}(\mu, \sigma)$ into an exponential distribution. Let $z \sim \text{Uniform}(0, 1)$ then, as described above:

$$g = \mu - \sigma \log(-\log z) \quad (17)$$

follows a Gumbel distribution with location μ and scale $\sigma > 0$. Now, consider the following monotonic transformation:

$$x = \exp\left(-\frac{g + \sigma \log \beta - \mu}{\sigma}\right) \quad (18)$$

$$= -\beta^{-1} \log(z). \quad (19)$$

Thus, $x \sim \text{Exponential}(\beta)$.

D Conventions & Implementation

Here we define some conventions and assumptions in our implementation.

D.1 Directed Graph Representation via Adjacency Matrices

As mentioned in the main text, we represent a directed graph with an adjacency matrix \mathbf{A} , where $A_{ij} = 1$ iff there is an arrow from node i to node j , i.e., $i \rightarrow j$ and $A_{ij} = 0$ otherwise. In the case of DAGs, this means that the matrix has zeros in its diagonal and $A_{ij} = 1$ implies $A_{ji} = 0$. Moreover, given a permutation in topological order (or reverse topological order) the adjacency matrix would have an upper triangular (or lower triangular) structure if one were to order the rows and columns according to that permutation.

D.2 Topological Order

A standard topological order given by a permutation vector $\pi = [\pi_1, \dots, \pi_D]$ defines constraints in a DAG such that arrows can only be drawn from left to right. For example, for the ordering $\pi = [2, 0, 1]$ the DAG $2 \rightarrow 0 \rightarrow 1$ is valid under such ordering but any DAG where, for example, arrows are drawn from 1 is invalid. Similarly, any DAG containing the link $0 \rightarrow 2$ is also invalid.

This places constraints on the set of *admissible* adjacency matrices under the given permutation. In particular, we are interested in representing this set via a distribution parameterized by a parameter matrix Θ , where $\Theta_{ij} > 0$ indicates that there is a non-zero probability of drawing a link $i \rightarrow j$. In this case, it is easy to see that the probability matrix Θ consistent with the permutation π satisfies $\Theta_{\pi_i \pi_j} = 0 \forall i > j$.

D.3 Reverse Topological Order

Analogously, in a reverse topological order given by permutation vector π , arrows can only be drawn from right to left. Thus, we see that the probability matrix consistent with the permutation π satisfies $\Theta_{\pi_i \pi_j}^r = 0 \forall i < j$.

D.4 Permutation Matrices

In order to express all our operations using linear algebra, which in turn allows us to apply relaxations and back-propagate gradients, we represent a permutation $\pi = [\pi_1, \dots, \pi_D]$ via a D -dimensional permutation matrix $\mathbf{\Pi}$ such as that $\mathbf{\Pi}_{ij} = 1$ iff $j = \pi(i)$ and $\mathbf{\Pi}_{ij} = 0$ otherwise. This means that we can recover the permutation π by computing the max over the columns of $\mathbf{\Pi}$, i.e., in Pythonic notation $\pi = \max(\mathbf{\Pi}, \dim = 1)$.

D.5 Distributions over DAGs

Let \mathbf{L} be a D -dimensional strictly lower diagonal matrix, i.e., $L_{ij} = 0, \forall i < j$ and $L_{ij} = 1$ otherwise. Similarly, let \mathbf{U} be a D -dimensional strictly upper diagonal matrix. Given a permutation matrix $\mathbf{\Pi}$ the corresponding DAG distributions are:

$$\Theta = \mathbf{\Pi}^\top \mathbf{U} \mathbf{\Pi}, \quad (20)$$

$$\Theta^r = \mathbf{\Pi}^\top \mathbf{L} \mathbf{\Pi}. \quad (21)$$

We will show this for the standard case of topological order. Consider Equation (20):

$$\Theta_{ij} = \sum_m \sum_k (\mathbf{\Pi}^\top)_{ik} U_{km} \mathbf{\Pi}_{mj} \quad (22)$$

$$= \sum_m \sum_k \mathbf{\Pi}_{ki} U_{km} \mathbf{\Pi}_{mj}. \quad (23)$$

this, for a given permutation π , we can express:

$$\Theta_{\pi_k \pi_m} = \mathbf{\Pi}_{k\pi_k} U_{km} \mathbf{\Pi}_{m\pi_m}, \quad (24)$$

which, as \mathbf{U} is an upper triangular matrix, implies $\Theta_{\pi_k \pi_m} = 0, \forall k > m$.

For clarity and consistency with previous literature, we emphasize our convention Θ_{ij} indicates the probability of a link $i \rightarrow j$. If we were to use the transpose definition of the space of adjacency matrices $\Phi = \Theta^\top$ indicating the probability of a link $\Phi_{ij} : j \rightarrow i$, as for example in [11], then we would have (in the case of a topological ordering) $\Phi = \mathbf{\Pi}^\top \mathbf{L} \mathbf{\Pi}$.

E The Relaxed Bernoulli Distribution

Here we follow the description in [23]. A random variable $A \in (0, 1)$ follows a relaxed Bernoulli distribution, also known as a binary Concrete distribution, denoted as $A \sim \text{RelaxedBernoulli}(\tau, \alpha)$ with location parameter $\alpha \in (0, \infty)$ and temperature $\tau \in (0, \infty)$ if its density is given by:

$$\text{RelaxedBernoulli}(a; \tau, \alpha) := p(a | \tau, \alpha) = \frac{\tau \alpha a^{-\tau-1} (1-a)^{-\tau-1}}{(\alpha a^{-\tau} + (1-a)^{-\tau})^2}. \quad (25)$$

For our purposes, we are interested in sampling from this distribution and computing the log probability of variables under this model. Below we describe how to do these operations based on a parameterization using Logistic distributions.

E.1 Sampling

Let us define the logistic sigmoid function and its inverse (the logit function) as

$$\sigma(x) := \frac{1}{1 + \exp(-x)}, \quad (26)$$

$$\sigma^{-1}(x) := \log \frac{x}{1-x}. \quad (27)$$

In order to sample $a \sim \text{RelaxedBernoulli}(\tau, \alpha)$ we do the following:

1. Sample $L \sim \text{Logistic}(0, 1)$
 - (a) $U \sim \text{Uniform}(0, 1)$
 - (b) $L = \log(U) - \log(1 - U)$
2. $b = \frac{\log \alpha + L}{\tau}$
3. $a = \sigma(b)$.

E.2 Log Density Computation

Given a realization b (before applying $\sigma(b)$), we also require the computation of its log density under the relaxed Bernoulli model. With the parameterization above using the Logistic distribution, it is easy to get this density by using the change-of-variable (transformation) formula to obtain:

$$\log p(b; \tau, \alpha) = \log \tau + \log \alpha - \tau b - 2 \log(1 + \exp(\log \alpha - \tau b)). \quad (28)$$

In order to obtain the log density of $0 < a < 1$ under the relaxed Bernoulli model, we need to apply the change of variable formula again, as $a = \sigma(b)$,

$$\log p(a; \tau, \alpha) = \log \tau + \log \alpha - \tau \sigma^{-1}(a) - 2 \log(1 + \exp(\log \alpha - \tau \sigma^{-1}(a))) - \log a - \log(1 - a). \quad (29)$$

E.3 Probability Re-parameterization

The relaxed Bernoulli distribution has several interesting properties described in [23]. In particular, the *rounding* property [23, Proposition 2], establishes that if $X \sim \text{RelaxedBernoulli}(\tau, \alpha)$:

$$\mathbb{P}(X > 0.5) = \frac{\alpha}{1 + \alpha}. \quad (30)$$

Therefore, our implementation adopts Pytorch parameterization using a "probability" parameter $\theta \in (0, 1)$ so that

$$\theta := \frac{\alpha}{1 + \alpha}. \quad (31)$$

F Relaxed Distributions over Permutations

We have seen that sampling from our distributions over permutations requires the `argsort` operator which is not differentiable. Therefore, in order to back-propagate gradients and estimate the parameters of our posterior over permutations, we relax this operator following the approach of [28],

$$\text{SoftSort}(\tilde{\mathbf{s}}) := \text{softmax} \left(\frac{\mathcal{L}_d(\text{sort}(\tilde{\mathbf{s}})\mathbf{1}^T, \mathbf{1}\tilde{\mathbf{s}}^T)}{\tau_\pi} \right), \quad (32)$$

where $\mathcal{L}_d(\cdot, \cdot)$ is a semi-metric function applied point-wise that is differentiable almost everywhere; τ_π is a temperature parameter; and $\text{softmax}(\cdot)$ is the row-wise softmax function. Here we have assumed that $\text{sort}(\tilde{\mathbf{s}}) := \text{sort}(\tilde{\mathbf{s}}, \text{descending}=\text{True})$, which applies directly to the Gumbel-Max construction. In the case of the Gamma construction, which assumes ascending orders, we simply pass in the negative of the corresponding scores. We note that Equation (32) uses $\text{sort}(\cdot)$, which unlike the `argsort` operation, is a differentiable operation.

F.1 Sampling

Sampling from our relaxed distributions over permutations is done by simply replacing the `argsort` operation used in the vanilla (hard) permutation distribution with the `SoftSort` function above. This function returns, in fact, a permutation matrix $\mathbf{\Pi}$ which is used as a conditioning value in the DAG distribution, as explained in Appendix D.5, and as input to the log probability computation in the KL term over permutations.

E.2 Log Probability Computation

The log probability of a permutation matrix Π given a distribution with parameters β (in the case of the Gamma construction) can be computed using Equation (1), where β_π are the permuted parameters given by:

$$\beta_\pi = \Pi\beta. \quad (33)$$

In the case of the Gumbel-Max construction, β_π is obtained by reversing the order of $s_\pi = \Pi s$.

G Full Objective Function Using Monte Carlo Expectations

We retake our objective function:

$$\begin{aligned} \mathcal{L} = & \mathbb{E}_{q_\pi(\pi | r, \beta)} [\log q_\pi(\pi | r, \beta) - \log p(\pi | r_0, \beta_0)] + \\ & \mathbb{E}_{q_\pi(\pi | r, \beta)q_{\mathcal{G}}(\mathcal{G} | \pi, \Theta)} (\log q_{\mathcal{G}}(\mathcal{G} | \pi, \Theta) - \log p(\mathcal{G} | \pi, \Theta_0)) + \\ & \mathbb{E}_{q_\pi(\pi | r, \beta)q_{\mathcal{G}}(\mathcal{G} | \pi, \Theta)} \sum_{n=1}^N \log p(\mathbf{x}^{(n)} | \mathcal{G}, \phi). \quad (34) \end{aligned}$$

H Additional Results

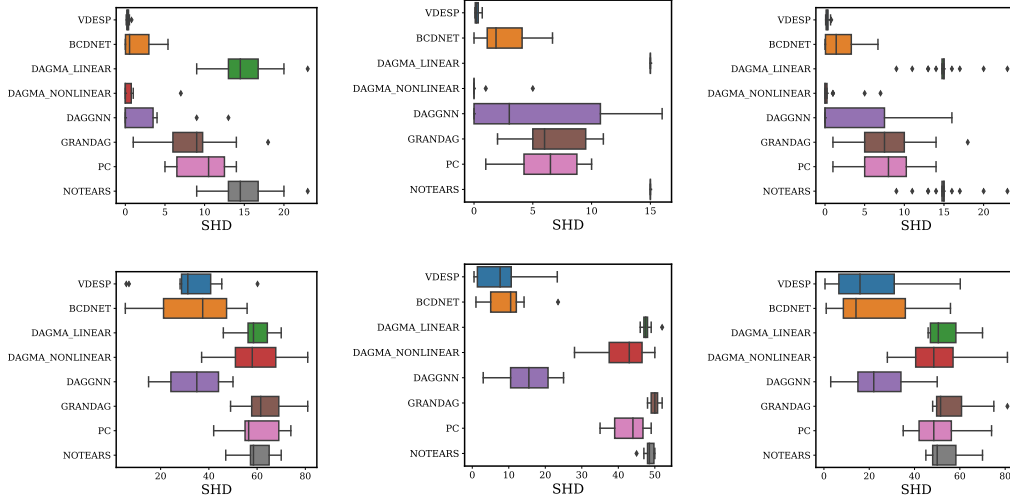


Figure 4: Results on the synthetic linear data with $D = 16$ variables (nodes) on ER (left), SF (middle), and all (right) graphs. The top row is with $E = 16$ edges and the bottom row with $E = 64$ edges, respectively.

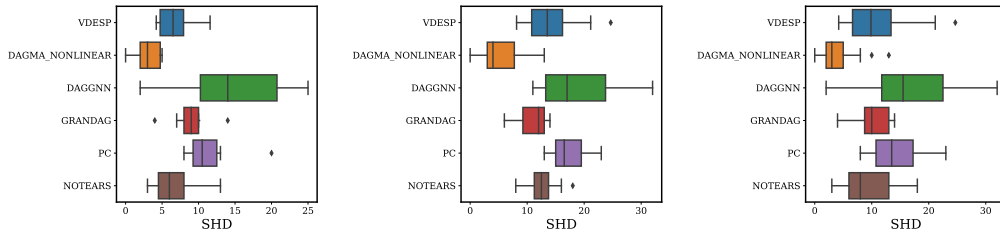


Figure 5: Results on the synthetic nonlinear data with $D = 16$ and $E = 16$ on ER (left), SF (middle), and all (right) graphs.

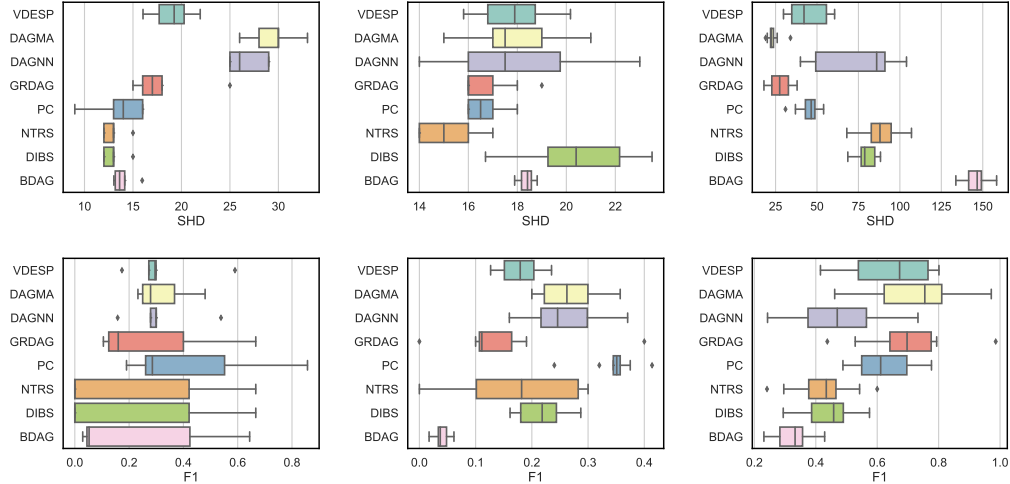


Figure 6: Results on real datasets: DREAM4 (Left), SACHS (middle) and SYNTREN (right). The top row shows the structural Hamming distance (SHD, the lower the better), while the bottom row shows the F1 score (the higher the better). The latter computed on the classification problem of predicting links including directionality.

I Additional Results on Alzheimer’s Data

We applied VDES for discovering the causal relationships between Alzheimer disease biomarkers and cognition. The source data were made publicly available by the Alzheimer’s Disease Neuroimaging Initiative (ADNI). These data have been used previously to evaluate causal discovery algorithms [31] because a “gold standard” graph for these data is known.

For our experiments we focused on 7 variables which include demographic information age (AGE) and years of education (PTEDUCAT) along with biological variables which include fludeoxyglucose PET (FDG), amyloid beta (ABETA) phosphorylated tau (PTAU), and the apolipoprotein E (APOE4) ϵ 4 allele. The last variable of interest represents the participant’s clinically assessed level of cognition (DX) indicating one of three levels: normal, mild cognitive impairment (MCI) and early Alzheimer’s Disease (AD). Ultimately, we want to infer the causal influences on DX.

The data is collected from participants as part of the first two phases of ADNI that commenced in 2003. In total, we have data for 1336 individuals after removing those with missing values.

The results are shown in Figures 7 and 8. We see that VDES uncovered the main underlying graph structure, while hinting at different explanations of the data which may require further investigation.

J VDES Hyper-Parameters and Reproducibility

In all our experiments we train our model by optimizing the ELBO using the Adam optimizer with learning rate 0.001. We set the temperature parameter of our relaxed permutation distributions to 0.5. The scores of the permutation distributions were set to give rise to uniform distributions and the posterior was initialized the the same values. We use Gaussians for the DAG distributions with zero mean prior and prior and initial posterior scales set to 0.1.

For the linear dataset we used 100 permutation samples and 100 DAG samples per permutation and optimize for 75000 iterations. For the synthetic non-linear data we set the number number of permutation samples = 2, number of DAG samples = 2 and training epochs = 30000 while we initialized the non-linear SEM noise scale = 1.0.

For the real data using the non-linear SEM we used a fixed noise scale = {0.01, 0.25, 0.3}, number of permutation samples = {10, 10, 5}, number of DAG samples = {15, 15, 5} and training epochs = {5000, 5000, 15000} for DREAM4, SACHS, and SYNTREN respectively.

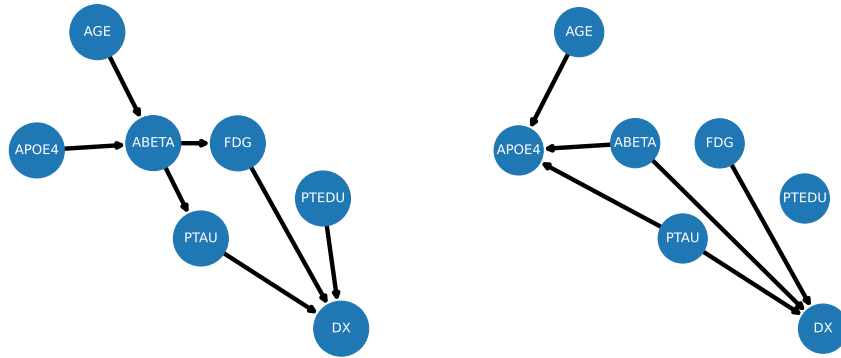


Figure 7: The true graph on the Alzheimer dataset (left) and the mean posterior graph predicted by VDESP.

In all cases when using a non-linear SEM, our model had a single hidden layer with 10 neurons and sigmoid activation.

For reproducibility purposes, we will make our code publicly available upon acceptance.

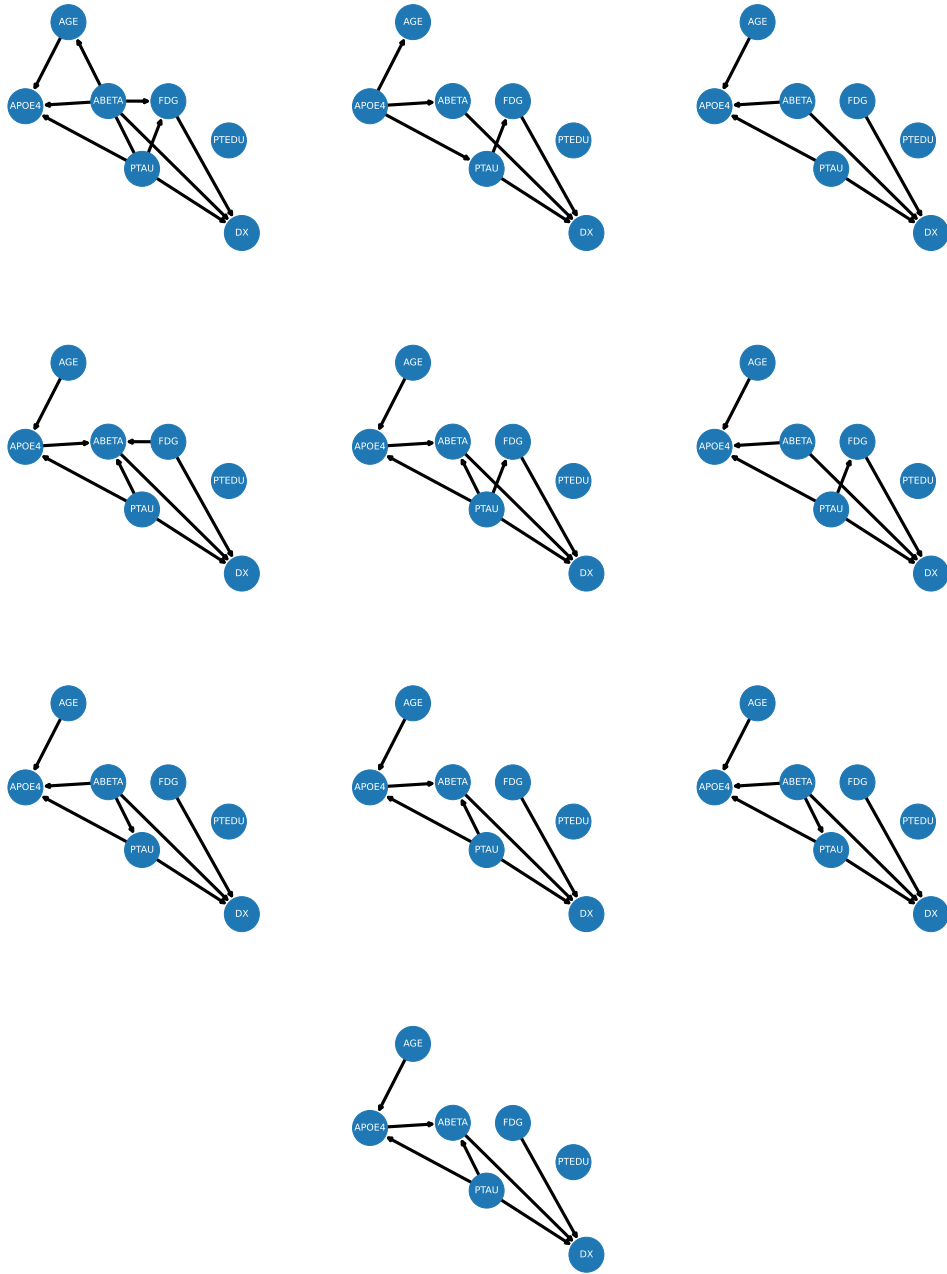


Figure 8: VDESP's Posterior samples on the Alzheimer dataset.